

Extrasolar planets and brown dwarfs around A–F type stars^{★,★★}

VII. θ Cygni radial velocity variations: planets or stellar phenomenon?

M. Desort¹, A.-M. Lagrange¹, F. Galland¹, S. Udry², G. Montagnier^{2,1}, H. Beust¹, I. Boisse³, X. Bonfils^{1,4}, F. Bouchy³, X. Delfosse¹, A. Eggenberger¹, D. Ehrenreich¹, T. Forveille¹, G. Hébrard³, B. Loeillet^{3,5}, C. Lovis², M. Mayor², N. Meunier¹, C. Moutou⁵, F. Pepe², C. Perrier¹, F. Pont⁶, D. Queloz², N. C. Santos^{2,4}, D. Ségransan², and A. Vidal-Madjar³

¹ Laboratoire d'Astrophysique de Grenoble, UMR5571 CNRS, Université Joseph Fourier, BP 53, 38041 Grenoble Cedex 9, France
e-mail: morgan.desort@obs.ujf-grenoble.fr

² Observatoire de Genève, Université de Genève, 51 Chemin des Maillettes, 1290 Sauverny, Switzerland

³ Institut d'Astrophysique de Paris, UMR7095 CNRS, Université Pierre & Marie Curie, 98bis boulevard Arago, 75014 Paris, France

⁴ Centro de Astronomia e Astrofísica da Universidade de Lisboa, Observatório Astronómico de Lisboa, Tapada da Ajuda, 1349-018 Lisboa, Portugal

⁵ Laboratoire d'Astrophysique de Marseille, UMR6110 CNRS, Université de Provence, BP 8, 13376 Marseille Cedex 12, France

⁶ Physikalisches Institut, University of Bern, Sidlerstrasse 5, 3012 Bern, Switzerland

Received 26 January 2009 / Accepted 27 July 2009

ABSTRACT

Aims. In the framework of the search for extrasolar planets and brown dwarfs around early-type main-sequence stars, we present the results obtained on the early F-type star θ Cygni.

Methods. ELODIE and SOPHIE at the Observatoire de Haute-Provence (OHP) were used to obtain 91 and 162 spectra, respectively. Our dedicated radial-velocity measurement method was used to monitor the star's radial velocities over five years. We also used complementary, high angular resolution and high-contrast images taken with PUEO at the CFHT.

Results. We show that θ Cygni radial velocities are quasi-periodically variable, with a ≈ 150 -day period. These variations are not due to the $\approx 0.35-M_{\odot}$ stellar companion that we detected in imaging at more than 46 AU from the star.

The absence of correlation between the bisector velocity span variations and the radial velocity variations for this $7 \text{ km s}^{-1} v \sin i$ star, as well as other criteria, indicate that the observed radial velocity variations do not stem from stellar spots. The observed amplitude of the bisector velocity span variations also seems to rule out stellar pulsations. However, we observe a peak in the bisector velocity span periodogram at the same period as the one found in the radial velocity periodogram, which indicates a probable link between these radial velocity variations and the low-amplitude lineshape variations with a stellar origin. Long-period variations are not expected from this type of star to our knowledge. If a stellar origin (hence of new type) were to be confirmed for these long-period radial velocity variations, this would have several consequences on the search for planets around main-sequence stars, both in terms of observational strategy and data analysis.

An alternative explanation for these variable radial velocities is the presence of at least one planet of a few Jupiter masses orbiting at less than 1 AU; however, this planet alone does not explain all observed features, and the θ Cygni system is obviously more complex than a planetary system with 1 or 2 planets.

Conclusions. The available data do not allow us to distinguish between these two possible origins. A vigorous follow-up in spectroscopy and photometry is needed to get a comprehensive view of the star intrinsic variability and/or its surrounding planetary system.

Key words. techniques: radial velocities – stars: early-type – stars: planetary systems – stars: individual: θ Cygni

1. Introduction

Radial-velocity (RV) surveys have led to the detection of more than 300 planets during the past decade¹. These surveys mainly focus on solar and later-type main-sequence (hereafter MS) stars ($\gtrsim F7$) that exhibit numerous lines with low rotational broadening, making them ideal targets for classical velocimetry. However, it is crucial to understand how planetary systems form over a wide variety of parent stars and to know, in particular, if there is a correlation between (*i*) the planet masses and

* Based on observations made with the ELODIE and SOPHIE spectrographs at the Observatoire de Haute-Provence (CNRS, France) and with the PUEO adaptive optics system at the Canada-France-Hawaii Telescope (CFHT), which is operated by the National Research Council of Canada, the Institut National des Sciences de l'Univers of the Centre National de la Recherche Scientifique of France, and the University of Hawaii.

** Tables of radial velocities are only available in electronic form at the CDS via anonymous ftp to cdsarc.u-strasbg.fr (130.79.128.5) or via <http://cdsweb.u-strasbg.fr/cgi-bin/qcat?J/A+A/506/1469>

¹ A comprehensive list of known exoplanets is available at <http://exoplanet.eu>.

the parent star masses as predicted, for instance, by [Kennedy & Kenyon \(2008\)](#), in order to constrain formation models such as those from [Ida & Lin \(2005\)](#) (but also [Boss 2006](#); and [Laughlin et al. 2004](#) for M dwarfs); and/or between (ii) the planet existence and the parent star masses. For massive stars, surveys of subgiant/giant stars have started to provide first information on planets at orbital distances typically greater than 0.7 AU (e.g., [Johnson et al. 2006, 2007](#); [Hatzes et al. 2005](#); [Niedzielski et al. 2007](#); [Lovis & Mayor 2007](#); [Sato et al. 2008](#)). Closer separations have to be investigated by observing massive main-sequence stars. In this framework, we have developed a tool dedicated to searching for planets around early (A–F) type stars. The method allowing measurement of the RV of rapid rotators is described by [Galland et al. \(2005a, hereafter Paper I\)](#).

In 2005 we started two surveys dedicated to searching for extrasolar planets and brown dwarfs around a volume-limited sample of A–F main-sequence stars *i*) with the ELODIE fiber-fed echelle spectrograph ([Baranne et al. 1996](#)) mounted on the 1.93-m telescope at the Observatoire de Haute-Provence (OHP, France) in the northern hemisphere; and *ii*) with the HARPS spectrograph ([Pepe et al. 2002](#)) installed on the 3.6-m ESO telescope at La Silla Observatory (Chile) in the southern hemisphere. In 2006, the ELODIE spectrograph was replaced by SOPHIE ([Bouchy et al. 2006](#)). We detected a planet around an F6V star with ELODIE ([Galland et al. 2005b, Paper II](#)) and a brown dwarf around an A9V star ([Galland et al. 2006b, Paper IV](#)), and with HARPS a two-planet system around an F6IV–V star ([Desort et al. 2008, Paper V](#)). We also derived the first statistics of planet existence around A–F stars thanks to our HARPS survey ([Lagrange et al. 2009, Paper VI](#)).

We present and analyse in this paper the RV variations of θ Cygni. Section 2 provides the stellar properties and the various data obtained on this object. In Sect. 3, we discuss the origin of the observed RV variations.

2. Stellar characteristics and measurements

The star θ Cygni (HD 185395, HIP 96441, HR 7469) is a $M_1 = 1.38 \pm 0.05 M_\odot$ star, with an age estimated at $1.5^{+0.6}_{-0.7}$ Gyr ([Nordström et al. 2004](#)), and located at 18.33 ± 0.05 pc from the Sun ([ESA 1997](#); [van Leeuwen 2007](#)). We took its rotational velocity $v \sin i$, effective temperature T_{eff} , and surface gravity $\log g$ from [Erspamer & North \(2003\)](#) and [Gray et al. \(2003\)](#) (values in Table 1). We assumed a spectral type F4V, commonly attributed to this star as, e.g., in the Bright Star Catalogue ([Hoffleit et al. 1991](#)) or in the HIPPARCOS catalogue ([ESA 1997](#)).

2.1. Spectroscopic data

2.1.1. Description of the data

Between 2003 and 2006, we recorded 91 high S/N spectra of θ Cygni with ELODIE and, between November 2006 and December 2008, we recorded 162 spectra with SOPHIE. The wavelength range is 3850–6800 Å for ELODIE and 3872–6943 Å for SOPHIE. Typical exposure times were 15 and 3 min for ELODIE and SOPHIE, respectively, leading to a S/N of ~ 200 . The exposures were performed with simultaneous-thorium spectra to follow and correct for the possible drift of the instrument due to local temperature/pressure variations (whose impact shows a standard deviation of 2.5 m s^{-1}). With SOPHIE we used the high-resolution ($R \approx 75\,000$) mode.

Table 1. θ Cygni stellar properties.

Parameter	θ Cygni
Spectral type	F4V
$v \sin i$ [km s ⁻¹]	7
V	4.49
$B - V$	0.395 ± 0.015
π [mas]	54.54 ± 0.15
Distance [pc]	18.33 ± 0.05
M_V	3.14
[Fe/H]	-0.08
T_{eff} [K]	6745
$\log g$	4.2
M_1 [M_\odot]	1.38 ± 0.05
Age [Gyr]	$1.5^{+0.6}_{-0.7}$
ppm (α) [†] [mas yr ⁻¹]	-8.15
ppm (δ) [†] [mas yr ⁻¹]	-262.99

[†] The proper motion is affected from the orbital motion that we discuss in Sect. 2.2.

Note: photometric and astrometric data from the HIPPARCOS catalogue ([ESA 1997](#); [van Leeuwen 2007](#)); spectroscopic data from [Nordström et al. \(2004\)](#) and [Erspamer & North \(2003\)](#).

2.1.2. Radial velocity variations

The radial velocities (Fig. 1) were measured using a dedicated tool (SAFIR) described in Paper I and based on the Fourier interspectrum method developed in [Chelli \(2000\)](#). The uncertainty associated with ELODIE data is 9 m s^{-1} on average, consistent with the value obtained from our simulations (see Paper I). In the case of SOPHIE data, the uncertainty is 5 m s^{-1} on average (taking the photon noise and instrument stability into account).

As θ Cygni has a relatively low projected rotational-velocity ($v \sin i = 7 \text{ km s}^{-1}$), we could also measure the RV using a Gaussian adjustment to the cross-correlation function (CCF). The results obtained by the two different methods are found to be consistent.

ELODIE and SOPHIE RV data show (Fig. 1) a quasi-periodic signal with peak-to-peak amplitude of about 220 m s^{-1} , much larger than the uncertainties. A drift in the RV curve moreover seems to be present over the whole data set, which could be attributed to a stellar companion (Sect. 2.2). We finally note that the amplitude of the RV variations could also be slightly variable.

We used the CLEAN algorithm ([Högbom 1974](#)), applied to Lomb-Scargle periodograms to derive the periodograms of the radial velocities measured with both instruments (Fig. 2). This algorithm removes the aliases associated with temporal sampling of the data, and it deconvolves the window function iteratively from the initial “dirty” periodogram to produce the resulting cleaned periodogram.

In the case of ELODIE data, the periodogram shows one peak at a period of 128 ± 5 days. The uncertainty is evaluated with the full width at half maximum of the highest peak. In the case of SOPHIE data, the peak corresponds to a period of 158 ± 10 days.

2.1.3. Line profile variations

SOPHIE Lomb-Scargle periodograms of the BVSs and curvatures (defined as in [Hatzes 1996](#)) are presented in Fig. 3, together with false-alarm probabilities (FAP, [Kürster et al. 1997](#)). In the case of the SOPHIE data, a peak is seen at approximately 140 days, i.e., not very different from the one measured in the

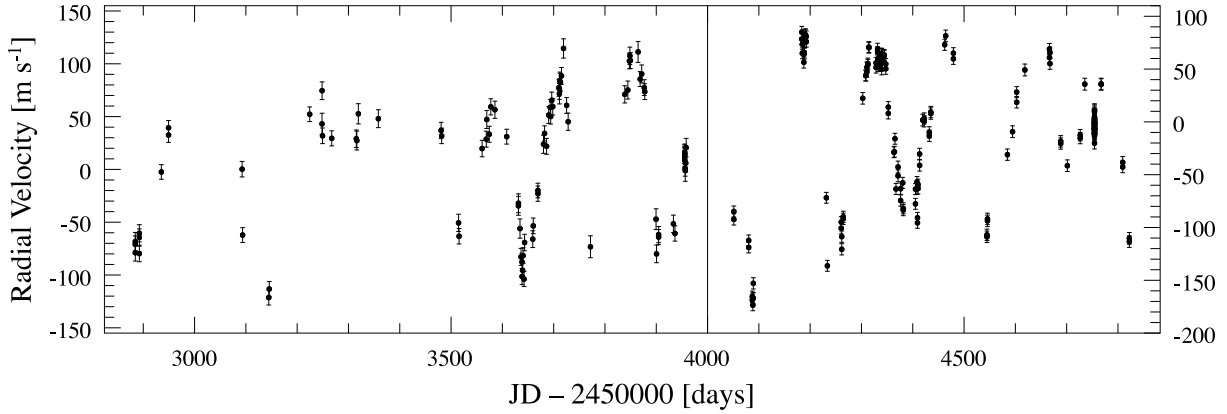


Fig. 1. Radial velocities of θ Cygni obtained with ELODIE (*left*) and SOPHIE (*right*).

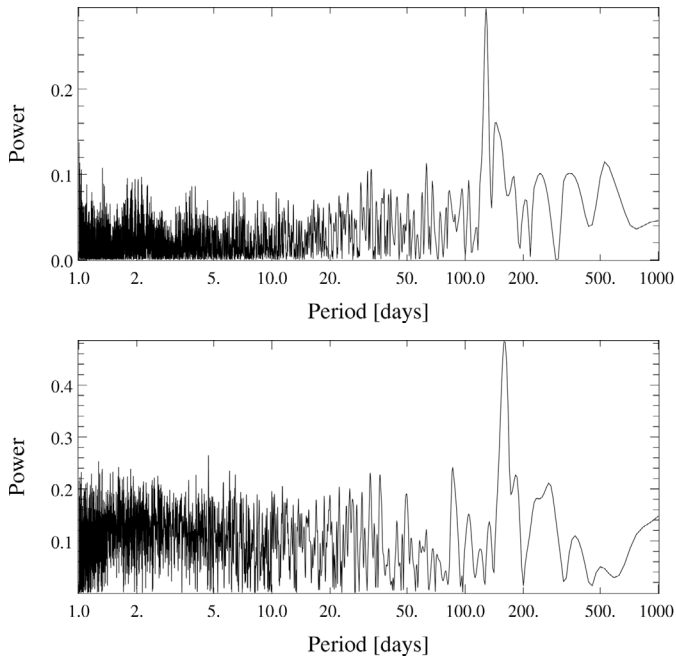


Fig. 2. ELODIE (*top*) and SOPHIE (*bottom*) CLEAN periodograms of the radial velocities. On each data set, one peak is observed, either at 128 ± 5 days or at 158 ± 10 days, respectively.

SOPHIE RV variations. No peak is detected on the still noisier ELODIE data.

Figure 4 presents the bisector velocity spans (BVSs) as a function of RVs for ELODIE and SOPHIE spectra. The amplitude of the BVS variations is quite small: 50 m s^{-1} , much smaller than the amplitude of the RV variations. No clear correlation is seen between the BVS and RV variations. It shows that the spectra are mainly shifted in radial velocity without significant changes in the line shape.

2.1.4. Stellar jitter

Finally, to quantify its short-term variations, we monitored θ Cygni for 1 h consecutively (as we did for HD 60532, Paper V). High-frequency variations are due to stellar phenomena and produce a noise (jitter) that has to be taken into account in the analysis of longer period variations. In October 2008, 46 consecutive spectra were then taken with SOPHIE under average observation conditions (airmass below 1.2, $S/N \approx 160$). The resulting RVs

and associated bisector velocity spans are presented in Fig. 5. It appears that the short-term variations can account for an RV amplitude of $\approx 30 \text{ m s}^{-1}$ ($\sigma_{\text{rv}} = 6.4 \text{ m s}^{-1}$) and that the total bisector velocity span amplitude over the whole SOPHIE data (Fig. 4, bottom) set can only be explained with those short-term variations. In the following attempt to analyse the high-amplitude RV variations, we adopt increased RV uncertainties (at least $\pm 6.4 \text{ m s}^{-1}$, fixed to that value) to take this stellar jitter into account.

2.2. Imaging data

We observed θ Cygni at high angular resolution and high contrast with the adaptive-optics (AO) instrument PUEO (Rigaut et al. 1998) mounted on the 3.6-m Canada-France-Hawaii Telescope (CFHT, USA). The near-infrared camera used, KIR (Doyon et al. 1998), has a field of view of $\sim 35'' \times 35''$, with a scale of $\sim 0.035''$ per pixel. We performed non saturated exposures, as well as 30-s saturated ones, to investigate the vicinity of the star at a deeper level. Special care was taken to ensure that the non saturated exposures could be used as references for accurately measuring the possible companions positions relative to the central star and as references for measuring the photometric contrast between the star and the possible companions.

The star θ Cygni was observed in June 2004, September 2005, and November 2007. The log of observations is given in Table 2. A classical reduction was performed using the software ECLIPSE (Devillard 1997). A candidate companion (CC) is seen in non saturated images (see Fig. 6) with the narrow bandwidth Fe II filter ($\lambda_0 = 1.644 \mu\text{m}$, $\Delta\lambda = 0.015 \mu\text{m}$). A deconvolution algorithm using the method described in Véran (1997) was applied to derive the contrast and angular separation (ρ) between the star and the companion.

Figure 7 shows the relative positions of the CC between 2004 and 2007. Clearly, the CC is not a background star, but it is bound to θ Cygni. Given the HIPPARCOS distance, 18.6 pc, we derive a projected separation of 46.5 AU between the two objects, thus a minimum period of roughly 230 years, assuming a circular orbit. Moreover, we see in Fig. 7 that the orbit of the companion is – still very partially – resolved over a three-year period of observation.

The measured contrast between θ Cygni and its companion θ Cygni B is $4.6 \pm 0.1 \text{ mag}$ in H band; in the K band, the measured contrast is $4.5 \pm 0.1 \text{ mag}$. Given the star’s apparent magnitudes, provided by Skrutskie et al. (2006), and distance (see above), we deduce H and K absolute magnitudes of 7.0 ± 0.1 and $6.7 \pm 0.1 \text{ mag}$, respectively. Using the BCA98 evolutionary

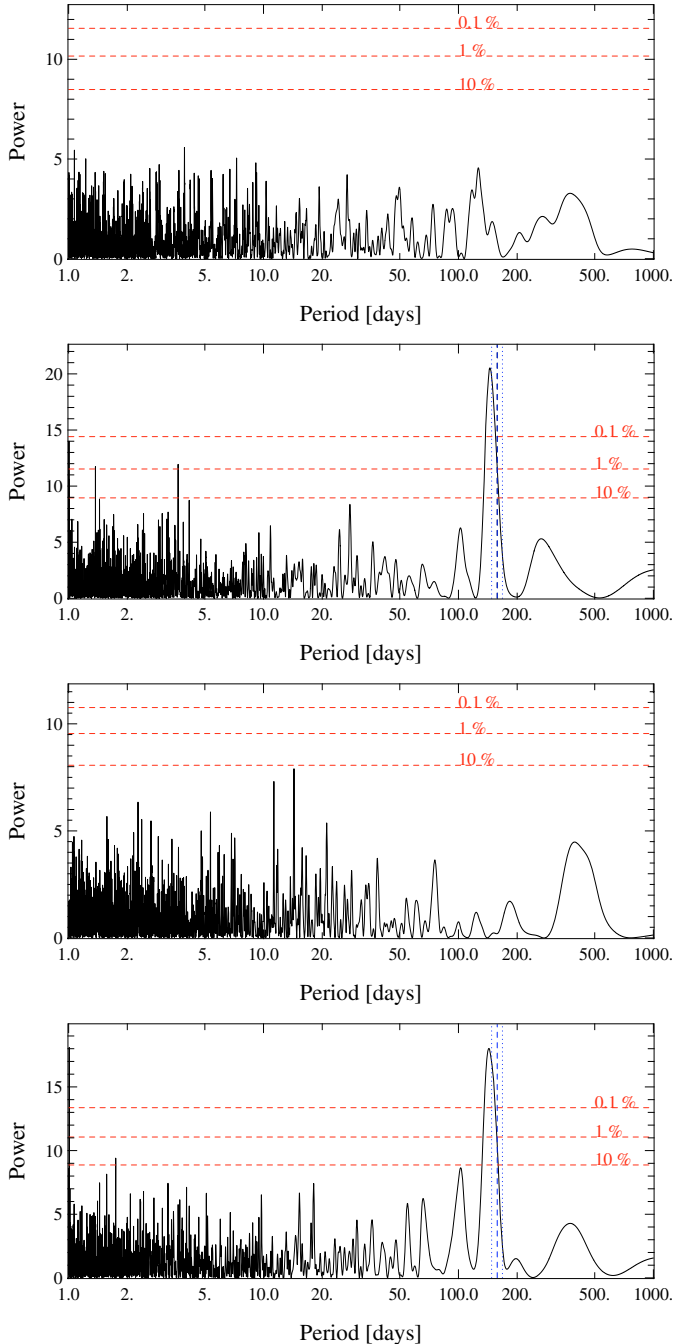


Fig. 3. ELODIE and SOPHIE Lomb-Scargle periodograms of the bisector velocity spans (*top 2 panels*) and curvatures (*bottom 2 panels*) with false alarm probabilities. On SOPHIE periodograms, the period of 158 ± 10 days is represented with vertical dashed lines (dotted for the ± 10 range).

models (Baraffe et al. 1998), and assuming any age above ~ 100 Myr, we deduce a mass $m_2 \approx 0.35 M_\odot$ for the companion. The evolutionary effects are negligible. Using the empirical relation given by Delfosse et al. (2000) for $M_H \approx 7$, we find a comparable mass $m_2 \approx 0.33 M_\odot$ for the companion.

The source θ Cygni was classified as a double star (Dommanget & Nys 1994). The Washington double star (WDS) data (Hartkopf & Mason 2001) indicate a visual companion detected several times since 1889, with a magnitude of ~ 12 , i.e., comparable to the visual magnitude expected from a $0.35 M_\odot$ star at θ Cygni distance. The relative position of this

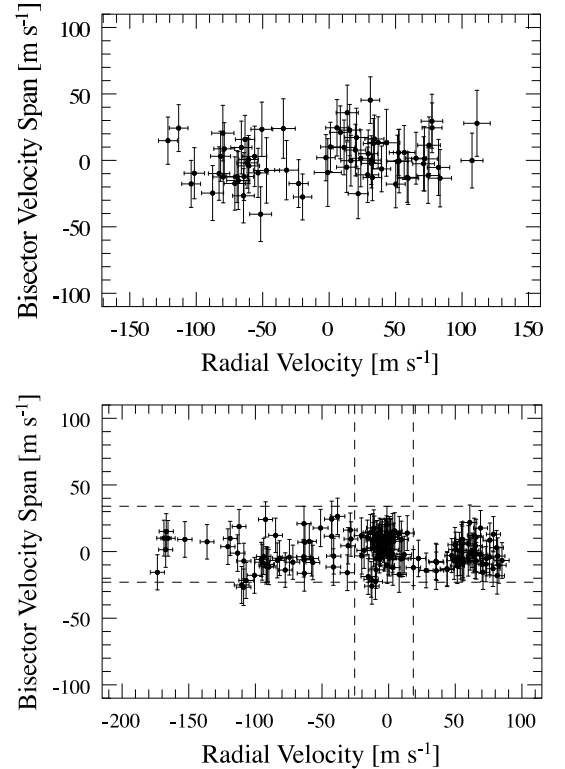


Fig. 4. Bisector velocity span versus RVs for ELODIE (*top*) and SOPHIE (*bottom*) data, showing that there is no correlation between line profiles and radial velocities. The dashed lines on SOPHIE data show the minimum effect of short-term variations, see Sect. 2.1.4.

Table 2. Log of WDS observations between 1889 and 1968 followed by the AO observations using PUEO at CFHT between June 2004 and November 2007.

Date	ρ [$''$]	θ [$^\circ$]	Contrast [mag]	Band
1889.37	3.62	43.9		
1892.38	3.79	47.0		
1898.46	3.37	49.2		
1898.63	3.71	46.9		
1958.58	3.42	51.7		
1968.72	2.92	59.9		
2004-06-28	2.510 ± 0.021	67.37 ± 0.48	4.6 ± 0.1	Fe II
2007-11-16	2.369 ± 0.005	69.02 ± 0.11	4.6 ± 0.1	Fe II

In the case of WDS data the uncertainties are unknown.

object varied between 1892 and 1968 (see Table 2), and indicates that this companion is bound to θ Cygni. The companion was not detected by HIPPARCOS because the contrast with θ Cygni was too high. It is reasonable to say that the WDS companion and the one found with PUEO is the same. Then we can track its motion over more than a century (Fig. 8), but its orbit is still very incomplete.

3. Origins of the observed RV variations

We investigate hereafter different possible origins for the RV variations: stellar phenomenon (spots, pulsations) and planets. Beforehand, we estimate the possible impact of the stellar companion on the spectroscopic data.

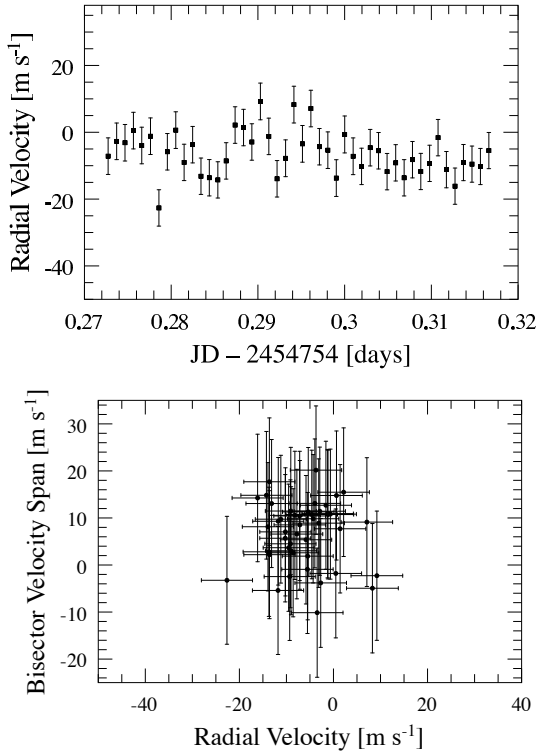


Fig. 5. *Top:* RVs for 1-h SOPHIE data. *Bottom:* bisector velocity spans versus RVs for 1-h SOPHIE data.

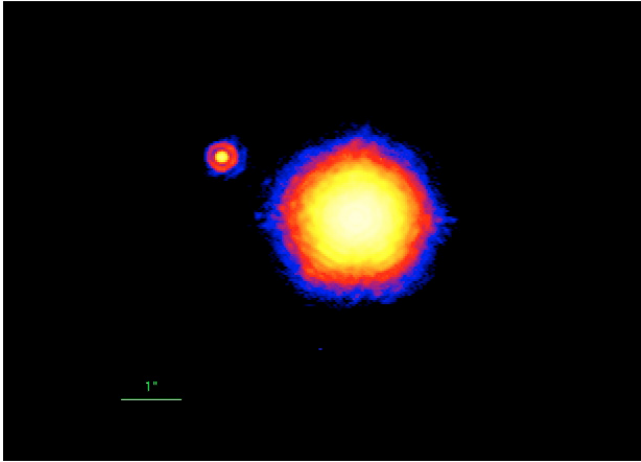


Fig. 6. High contrast and angular resolution image acquired with the adaptive optics system PUEO installed at CFHT: a companion is clearly visible.

3.1. Impact of the stellar companion on the RV data

The star θ Cygni B could a priori play a role on the measured radial velocities in two ways. Firstly, given their separation ($\approx 2''$) and given the usual seeings and the entrance width of the optical fiber, the spectra of the two stars are superimposed in the ELODIE or SOPHIE data (fiber entrance of $2''$ and $3''$, respectively). This could introduce a bias in the measurements. However, the contrast of 4.6 mag in H band translates into a contrast of 7.9 mag (a flux ratio of ~ 1500) in the V band, hence the negligible signal of the secondary in our spectra. We expect a radial-velocity effect below 1 m s^{-1} . If very active, it could still produce a weak $H\alpha$ signature superimposed on the

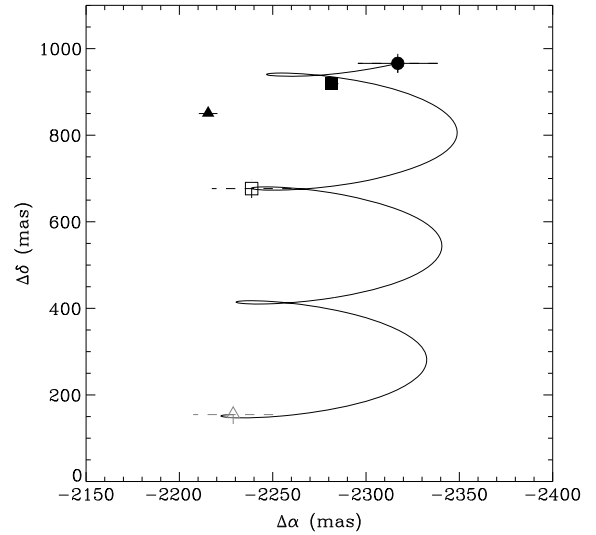


Fig. 7. Temporal evolution of the separation of the stellar companion of θ Cygni with respect to the central star. Filled symbols represent the position of the stellar companion relative to the main star for the three AO observations (*filled circle:* June 2004; *filled square:* September 2005; *filled triangle:* November 2007), whereas empty symbols show the positions at the same dates in case of a background star. The curve shows the path that would have followed the candidate companion if it was a background star, taking the star proper- and parallactic-motion into account.

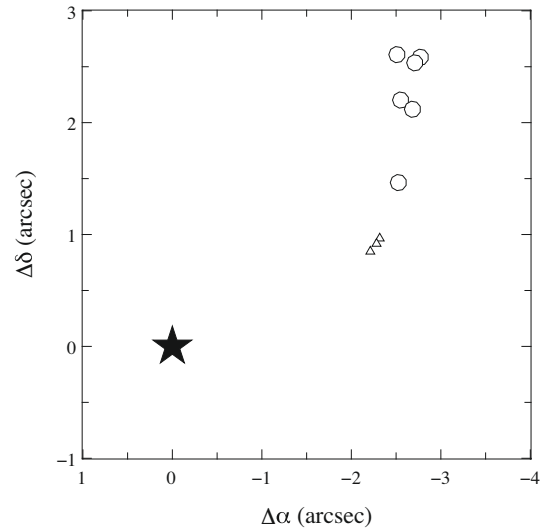


Fig. 8. Positions of the companion star with respect to the primary star for more than one century. The star represents the primary θ Cygni, the circles the WDS data (uncertainties are unknown), and the triangles our AO data (uncertainties are smaller than the symbols).

θ Cygni $H\alpha$ line. This does not affect our results, as this line is not considered in the RV measurements.

With the classical cross-correlation technique, the potential pollution of the spectrum by a stellar companion can be tested using various masks. We therefore checked that the RV amplitudes remain identical when using various masks. Also, the RVs are identical if we use either the red part or the blue part of the spectra to measure them. This confirms that the spectrum of the companion has no impact on the measured radial velocities.

Secondly, the stellar companion of course induces radial velocity variations in the primary. Given the companion properties and assuming the system seen edge-on, we estimate the

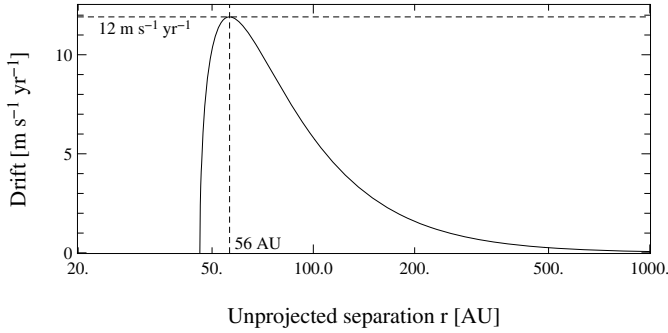


Fig. 9. Possible drift induced by the stellar companion given the unprojected true separation r to the primary star.

maximum drift possibly induced on the primary star by plotting the acceleration projected on the line of sight z , with respect to the true separation r (Fig. 9)

$$\frac{d^2z}{dt^2} = \frac{Gm_2}{r^2} \cos \left[\arcsin \left(\frac{\rho}{r} \right) \right],$$

where G is the gravitational constant, $m_2 = 0.35 M_\odot$ the mass of the secondary, and $\rho = 46$ AU the closest projected separation measured. We find a maximum drift of $12 \text{ m s}^{-1} \text{ yr}^{-1}$, which would lead to a maximum drift of 60 m s^{-1} over 5 years. In fact, a similar drift has to be included in our fit of the radial-velocity curve (see Sect. 3.3). The star θ Cygni B could then explain such a drift, but of course the observed periodic radial-velocity variations with an amplitude larger than 150 m s^{-1} are not explained by the presence of this stellar companion.

3.2. Stellar phenomenon

3.2.1. Stellar spots

We saw in the previous section that there is no correlation between the star RV variations and the BVS variations. Given the star's projected rotational-velocity, the instrument resolution, and according to the study presented in Desort et al. (2007), we can definitely conclude that the observed RV variations are not due to stellar spots. Indeed, were this the case, a correlation between the BVS and the RV would be observed. Typically, given the star's properties, one or more spots on an inclined star would be needed to reproduce a periodic signal, and a linear correlation coefficient $\simeq -0.5$ between the bisector velocity spans and the RVs. Given the observed RV amplitude, the amplitude of the BVS would therefore be much higher than what is actually observed.

Also, in such a case, one would expect significant photometric variations. A single spot producing such an RV variation would induce a photometric amplitude between 5 and 30 mmag, depending mainly on the star inclination and the spot location (Desort et al. 2007). The photometry given by HIPPARCOS (ESA 1997) is constant with a scatter of only 0.004 mag. We recognize, however, that the HIPPARCOS data were not recorded simultaneously with the spectroscopic ones, so this photometric argument is certainly weaker than the absence of correlation between RV and BVS variations. No clear emission in the core of the Ca II lines is observed (see Fig. 10 for the Ca II K line) which excludes a high level of activity.

We looked for possible long-term stellar variations using classical $H\alpha$, β , γ indicators. Very faint $H\alpha$ variations are detected, but they are not correlated with the RV variations. As

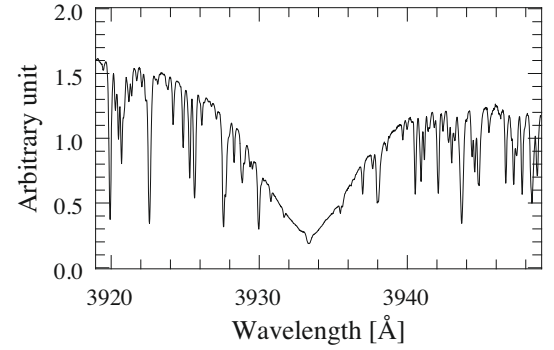


Fig. 10. No emission is observed in the Ca II K line for the θ Cygni spectra. This is the average spectrum of all the SOPHIE spectra used, after recentering by the RV variations measured.

the $H\alpha$ indexes are moreover quite sensitive to pollution by the thorium lamp, we cannot attribute them to a stellar origin.

Finally, the stellar rotational period is less than 7 days according to its $v \sin i$ and assuming a stellar radius typical for this type of star, a spot or a set of spots cannot explain RV variations with periods of one hundred days or more. We can therefore safely conclude that spots are most probably not responsible for the observed RV variations.

3.2.2. Granulation

Another source of variation could be the attenuation or suppression of the convective blueshift due to the presence of plages (e.g., Deming & Plymate 1994; Marquez et al. 1996). The expected convective blueshift expected for θ Cygni would be in the range $400\text{--}800 \text{ m s}^{-1}$ depending on the line (see Gray 2009 for a F5IV–V, which is the closest to θ Cygni in his sample). The observed variations could then be due to a cyclic variation with a plage filling factor varying between 0 and 30%, typically in order to produce the 220 m s^{-1} variation. However, such a variation of the convection properties should lead to a strong variation in the bisectors and in the Ca II index, which is not the case.

3.2.3. Stellar pulsations

Generally, pulsations induce line-profile variations that strongly affect the bisector velocity span (Paper VI). Besides, the timescale of the observed radial-velocity variations (≥ 100 days) is far larger than the ones of pulsations known for this type of main-sequence stars. It is in fact more characteristic of giant stars variability. Variability periods of a few days are observed in the case of the pulsating γ Doradus stars (Mathias et al. 2004). Moreover, if we integrate the RVs measured between a minimum and a maximum of the amplitude for half a period, we end up with a total displacement close to the stellar radius, which, if even possible, would lead to detectable photometric variations.

It is therefore unlikely that classical pulsations are responsible for the observed RV variations. However, the presence of a peak at about 150 days in the BVS periodogram and in the RV periodogram indicates that the period of the RV variations is linked in some way to the low amplitude line shape variations. Such a situation has never been reported to our knowledge and is indeed quite puzzling. We cannot at this stage exclude that we could be facing a new type of stellar variability, undetected so far because of a lack of long-term, very-precise RV monitoring of main-sequence stars.

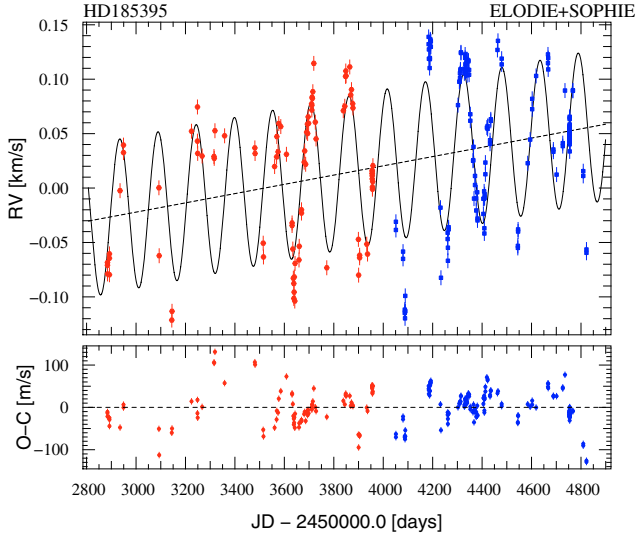


Fig. 11. ELODIE and SOPHIE radial velocities and orbital solution for θ Cygni, with one planet ($2.3 M_{\text{Jup}}$ at ~ 0.6 AU, circular orbit) and a drift. The residuals to the fitted orbital solution are displayed below.

3.3. Planet(s) around θ Cygni

The θ Cygni RV curve shows quasi-periodic variations with a period of ~ 130 – 150 days, together with a variable positive trend. Moreover, the RV curve seems to be modulated in amplitude. We now try to see whether these variations can be attributed to a planet or a planetary system.

We first tried to fit the whole data set (with uncertainties set to $\pm 6.4 \text{ m s}^{-1}$) assuming a single planet and allowing a drift. We failed to correctly reproduce the observed RVs. Figure 11 shows an example of a fit with a planet on a circular orbit (plus a drift). The planet that produces such an RV curve has a mass of $2.3 M_{\text{Jup}}$ and is on a 0.6 AU circular orbit (Table 3). The algorithm ends up with a period of 155 days hung on the SOPHIE data set, but fails to properly fit the ELODIE data set, as if there was period/phase change with time (clearly visible as structure in the residuals near the range [3600–3800] days). The additional drift needed is $16 \text{ m s}^{-1} \text{ yr}^{-1}$, slightly higher than the maximum value that the binary companion would probably produce. We note that a system that fails to fit satisfactorily the *whole* set of data (taken over more than 5 years) would allow the data to be fitted if they were limited to one or two consecutive periods.

We then tried to simultaneously fit the whole set of data, assuming the presence of several planets and using a genetic algorithm search. No stable solution was found. The only satisfactory fits are achieved by unstable systems with orbits that cross each other. We show an example in Fig. 12 of a fit obtained with a two-companion plus drift model. The residuals are still very high, the fit is not improved compared to the one-companion plus drift model (residual rms 35 m s^{-1} versus 39 m s^{-1} , and the drift that we get is approximately the same: $17 \text{ m s}^{-1} \text{ yr}^{-1}$ versus $16 \text{ m s}^{-1} \text{ yr}^{-1}$). Moreover, these kinds of configurations with massive planets on such close orbits are not dynamically stable.

The system is then obviously more complex than just consisting of one, two, or even three planets plus a drift. We then explored more exotic configurations:

- instead of harbouring one single planet, the system could consist of a binary planet system orbiting the star, much like the Pluto–Charo system, but with higher masses. However, the radial-velocity signal generated by this configuration would be very close to the one generated by a single planet

Table 3. ELODIE/SOPHIE best orbital solution for θ Cygni, considering one planet and a drift.

Parameter		θ Cygni <i>b</i>
P	[days]	154.5 ± 0.4
T_0	[JD–2 450 000]	4016 ± 1
e		0 (fixed)
ω	[deg]	0
K	[m s^{-1}]	70 ± 4
N_{meas}		253
$\sigma_{\text{O-C}}$	[m s^{-1}]	38.7
reduced χ^2		6.1
$a_1 \sin i$	[10^{-3} AU]	0.99
$f(m)$	[$10^{-9} M_{\odot}$]	5.5
M_1	[M_{\odot}]	1.38
$m_2 \sin i$	[M_{Jup}]	2.29
a	[AU]	0.63
drift	[$\text{m s}^{-1} \text{ yr}^{-1}$]	16 ± 4

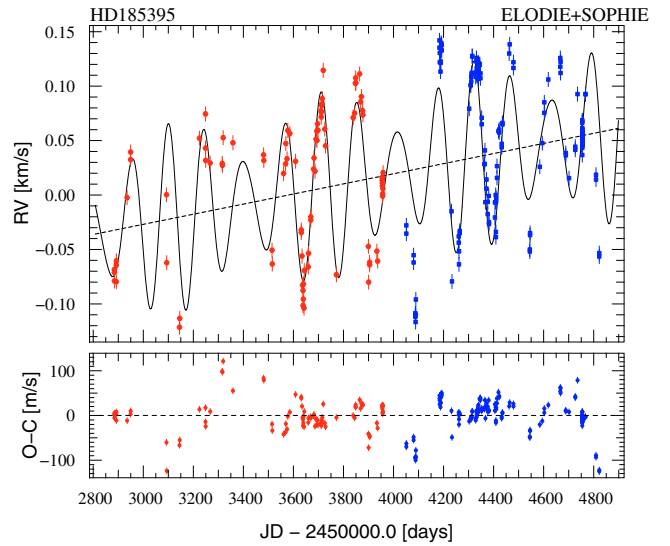


Fig. 12. ELODIE and SOPHIE radial velocities and orbital solution for θ Cygni, with two planets ($2.1 M_{\text{Jup}}$ at ~ 0.6 AU and $0.8 M_{\text{Jup}}$ at ~ 0.5 AU on circular orbits) and a drift. The residuals to the fitted orbital solution are displayed below.

having the total mass. The only departure from the pure Keplerian system would be related to the secular perturbations of the orbit due to the binary nature of the system. The associated secular period would be at least several hundred primary orbital periods, i.e., much longer than our observation time span; hence, we should mainly detect the primary orbital signal with good accuracy;

- one could also think of 2 co-orbiting planets locked in 1:1 mean-motion resonance. Such a configuration has been observed in the system of Saturn satellites. The two satellites orbit Saturn on the same orbit. In the rotating frame, they have synchronized horseshoe-like libration motions that prevent them from colliding. The less massive one has the largest amplitude motion (Yoder et al. 1983). The associated libration period is here again a few hundred orbital periods of the primaries. Over a shorter time span, the radial-velocity signal of the whole system will mainly consist of the sum of the individual signals of the two planets. If we assume that the two planets have zero eccentricities, the radial velocity signal will have the form $A \cos(nt) + B \cos(nt + \phi)$, where n is the common mean motion of the two planets, A and B

are amplitudes related to the masses of the planets, and ϕ is a phase shift that depends on their current mutual configuration. This can be rewritten as $C \cos(nt + \psi)$ where C and ψ are new amplitudes and phases that depend on A , B , and ϕ . This is equivalent to the signal generated by one single planet. This remains true if the planets have small eccentricities, and if they have larger eccentricities, the mutual system is not stable. Here again, the only departure from this signal will be the temporal variation of C and ψ that is related to the mutual libration motion of the two bodies. Hence we should not expect to see changes before several decades. The signal detected over our observation timespan should not be different from that of a single planet.

4. Concluding remarks

The radial velocities obtained with ELODIE and SOPHIE on θ Cygni are quasi-periodically variable, with a ≈ 150 day period. We investigated different possible origins to these RV variations, either star or planet related.

Given knowledge today of stellar activity, using several criteria as usual in this type of study, we are unable to attribute these variations to the star itself (spots, pulsations); however, the peak in the periodogram of the BVSs at ≈ 140 days, i.e., close to the period of the RV variations prevents us from totally excluding a stellar origin.

We tried to fit the data with one planet orbiting at less than 1 AU and with a mass of a few Jupiter masses, also taking the impact of the observed companion star into account. It appears that such an hypothesis allows us to fit only part of the data, recorded over a limited number of periods, but fails to satisfactorily fit the whole set of data (taken over more than 5 years). More complex systems were investigated, but no convincing result was obtained. More observations and detailed studies of gravitational interaction between the 2 planets are needed to understand this system.

With the data available, we are then not able to conclude on the origin of these puzzling RV variations. If a planet origin is confirmed, then θ Cygni, with a spectral type of F4V, would be the earliest main-sequence star hosting planets found so far. Moreover, it would be one of the few low-metallicity stars hosting planets. Its planetary system would not be simple, and it would in particular include strongly interacting planets.

If a stellar origin were confirmed, then this would show that, unexpectedly, some main-sequence stars, not classified as active by the usual criteria (e.g., Ca II H&K indexes) or pulsating, may undergo intrinsic variations that produce quasi-periodical, large-amplitude, and long-period (more than 100 days) RV variations, with at the same time, low levels of line shape deformations (hence small-amplitude BVS variations). Such situations have not been considered so far in the analysis of RV variations, and would need to be considered in future searches for such long-period planets, both in terms of observational strategy and data analysis.

We can at least conclude that θ Cygni is an individual complex system that deserves many more observations to be understood, and it may also serve as an example for other searches.

Acknowledgements. We acknowledge support from the French CNRS and the support from the Agence Nationale de la Recherche (ANR grant NT05-4_44463). We are grateful to the Observatoire de Haute-Provence (OHP) and the

CFHT for their help during the observations, and to the Programme National de Planétologie (PNP, INSU).

These results have made use of the SIMBAD database, operated at the CDS, Strasbourg, France. They also make use of data products from the Two Micron All Sky Survey, which is a joint project of the University of Massachusetts and the Infrared Processing and Analysis Center/California Institute of Technology, funded by the National Aeronautics and Space Administration and the National Science Foundation.

We also thank Gérard Zins and Sylvain Cêtre for their help in implementing the SAFIR interface.

X.B. acknowledges support from the Fundação para a Ciência e a Tecnologia (Portugal) in the form of a fellowship (reference SFRH/BPD/21710/2005) and a programme (reference PTDC/CTE-AST/72685/2006), as well as the Gulbenkian Foundation for funding through the “Programa de Estímulo à Investigação”.

N.C.S. would like to acknowledge the support from Fundação para a Ciência e a Tecnologia (Portugal) in the form of a grant (references POCI/CTE-AST/56453/2004 and PPCDT/CTE-AST/56453/2004), and through programme Ciência 2007 (C2007-CAUP-FCT/136/2006).

References

- Baraffe, I., Chabrier, G., Allard, F., & Hauschildt, P. H. 1998, *A&A*, 337, 403
 Baranne, A., Queloz, D., Mayor, M., et al. 1996, *A&A*, 119, 373
 Bouchy, F., & the SOPHIE team 2006, SOPHIE: the Successor of the Spectrograph ELODIE for Extrasolar Planet Search and Characterization, in Tenth Anniversary of 51 Peg-b: status of and Prospects for Hot-Jupiter Studies, Colloquium held at OHP, France, August 22–25, 2005, ed. L. Arnold, F. Bouchy, & C. Moutou (Paris: Frontier Group), 319
 Boss, A. P. 2006, *ApJ* 643, 501
 Chelli, A. 2000, *A&A* 358, L59
 Delfosse, X., Forveille, T., Ségransan, et al. 2000, *A&A*, 364, 217
 Deming, D., & Plymate, C. 1994, *ApJ*, 426, 382D
 Desort, M., Lagrange, A.-M., Galland, F., et al. 2007, *A&A*, 473, 983
 Desort, M., Lagrange, A.-M., Galland, F., et al. 2008, *A&A*, 491, 883
 Devillard, N. 1997, *The Messenger*, 87
 Dommanget, J., & Nys, O. 1994, *Com. de l’Observ. Royal de Belgique*, 115, 1
 Doyon, R., Nadeau, D., & Vallee, P. 1998, *SPIE*, 3354, 760D
 Erspamer, D., & North, P. 2003, *A&A*, 398, 1121
 Galland, F., Lagrange, A.-M., Udry, S., et al. 2005a, *A&A*, 443, 337
 Galland, F., Lagrange, A.-M., Udry, S., et al. 2005b, *A&A*, 444, L21
 Galland, F., Lagrange, A.-M., Udry, S., et al. 2006a, *A&A*, 447, 355
 Galland, F., Lagrange, A.-M., Udry, S., et al. 2006b, *A&A*, 452, 709
 Gray, D. F. 2009, *ApJ*, 697, 1032G
 Gray, R. O., Corbally, C. J., & Garrison, R. F. 2003, *AJ*, 126, 2048
 Hartkopf, W. I., & Mason, B. D. 2001, *BAAS*, 33, 1194
 Hatzes, A. P. 1996, *PASP*, 108, 839
 Hatzes, A. P., Guenther, E. W., Endl, M., et al. 2005, *A&A*, 437, 743
 ESA 1997, *The Hipparcos and Tycho Cat*, ESA SP-1200
 Hoffleit, D., & Warren, Jr., W. H. 1991, *Bright Star Catalogue* (5th Revised edn.), NSSDC/ADC
 Högbom, J. A. 1974, *A&AS*, 15, 417
 Ida, S., & Lin, D. N. C. 2005, *ApJ*, 626, 1045I
 Johnson, J. A., Marcy, G. W., Fisher, D. A., et al. 2006, *ApJ*, 652, 1724
 Johnson, J. A., Butler, R. P., Marcy, G. W., et al. 2007, *ApJ*, 665, 785
 Kennedy, G. M., & Kenyon, S. J. 2008, *ApJ*, 673, 502
 Kürster, M., Schmitt, J. H. M. M., Cutispoto, G., & Dennerl, K. 1997, *A&A*, 320, 831
 Lagrange, A.-M., Desort, M., Galland, F., et al. 2009, *A&A*, 495, 335
 Laughlin, G., Bodenheimer, P., & Adams, F. C. 2004, *ApJ*, 612, 73
 Lovis, C., & Mayor, M. 2007, *A&A*, 472, 657
 Márquez, I., Bonet, J. A., & Vázquez, M. 1996, *A&A*, 306, 305
 Mathias, P., Le Contel, J.-M., & Chapellier, E. 2004, *A&A*, 417, 189
 Niedzielski, A., Konacki, M., Wolszczan, A., et al. 2007, *ApJ*, 669, 1354
 Nordström, B., Mayor, M., Andersen J., et al. 2004, *A&A*, 418, 989
 Pepe, F., Mayor, M., Rupprecht, G., et al. 2002, *The ESO Messenger*, 110, 9
 Rigaut, F., Salmón, D., & Arsenault, R. 1998, *PASP*, 110, 152R
 Sato, B., Izumiura, H., Toyota, E., et al. 2008, *PASJ*, 60, 539
 Skrutskie, M. F., Cutri, R. M., Stiening, R., et al. 2006, *AJ*, 131, 1163
 van Leeuwen, F. 2007, *A&A*, 474, 653
 Vêran, J. P. 1997, Ph.D. Thesis, École Nationale Supérieure des Télécommunications
 Yoder, C. F., Colombo, G., Synnott, S. P., & Yoder, K. A. 1983, *Icarus*, 53, 431